A mobile system for precise wireless pulse transit time (PTT) monitoring

A. Weder, M. Pietzsch, Sebastian Zaunseder, M. Zimmerling, S. Netz

A Mobile System for Precise Wireless Pulse Transit Time (PTT) Monitoring

A. Weder
Fraunhofer IPMS
Maria-Reiche-Str. 2
Dresden, Germany
weder@ipms.
fraunhofer.de

M. Pietzsch
Fraunhofer IPMS
Maria-Reiche-Str. 2
Dresden, Germany
pietzsch@ipms.
fraunhofer.de

S. Zaunseder
Fraunhofer IPMS
Maria-Reiche-Str. 2
Dresden, Germany
zaunseder@ipms.
fraunhofer.de

M. Zimmerling
Fraunhofer IPMS
Maria-Reiche-Str. 2
Dresden, Germany
zimmerling@ipms.
fraunhofer.de

S. Netz
Fraunhofer IPMS
Maria-Reiche-Str. 2
Dresden, Germany
netz@ipms.
fraunhofer.de

ABSTRACT

The pulse transit time (PTT) is a parameter which can be used to characterize the functional state of the cardiovascular system. The PTT, which is closely connected to the blood pressure, can be derived from an electrocardiogram (ECG) and a simultaneously recorded photoplethysmogram (PPG) signal. In contrast to conventional non-invasive blood pressure measurements, the PTT can be calculated quasi continuously, giving instant feedback to condition changes. Many proposed systems use cables to connect ECG and PPG sensors. This is sufficient for stationary applications. This paper presents a system for wireless PTT measurements that permits patient mobility and thus makes new application scenarios possible. The main challenge of wireless time synchronization, necessary for precise PTT results, is solved using the IEEE 802.15.4 beacon enabled mode.

Categories and Subject Descriptors

J.3 [**Life and Medical Sciences**]: Health; C.2.1 [**Computer-Communication Networks**]: Network Architecture and Design—*Wireless communication*; I.2.1 [**Artificial Intelligence**]: Applications and Expert Systems—*Medicine and science*

General Terms

Algorithms

Keywords

PTT, ECG, PPG, IEEE 802.15.4, wireless, wavelet transform

1. INTRODUCTION

Chronic hypertension (elevated arterial blood pressure) is an important risk factor for heart attacks and strokes. Therefore, the monitoring of the *blood pressure* (BP) is an essential measure of preventive medical examination. Especially long term monitoring during a whole day or even week is of high medical relevance.

The current practice of conventional non-invasive BP measurement is the sphygmomanometer (blood pressure meter). This device uses a cuff to restrict the blood flow at the patient's arm and a manometer to measure the pressure. Automatic systems determine the pressure at what the blood flow is just starting by oscillometric detection. One of the main drawbacks of these cuff based systems is the limitation to discrete BP measurements in intervals of 15 minutes during the daytime and 30 minutes during the night [4, p. 90]. They can not be used for continuous measurements to track short time variations.

The most accurate way of recording the BP continuously is the invasive measurement. Thereby, the pressure within the artery is directly measured using a fluid filled system and a pressure-sensing transducer [10, p. 58]. In practice, this method is not applicable for long term monitoring due to intense restriction for the patients (e.g. risk of artery thrombosis) and the limitation to clinical applications.

Thus, alternative parameters which can be recorded without these restrictions are given precedence. A commonly used method for non-invasive beat-by-beat BP estimation is based on the *Pulse Transit Time* (PTT) [6, 7, 13].

The PTT is the time difference between drive out of the blood from the heart and the arrival of the generated blood pressure wave at a distal point of the body. The PTT varies inversely with blood pressure.

Several studies can be found assuming a linear correlation between PTT and systolic BP [6]. While Payne et al.

rate the PTT in [23] as an unreliable parameter for direct BP calculations, it might be useful to record and investigate BP variations on an individual basis [5]. One of the main challenges for BP estimation is the calibration [19]. Besides BP calculation, the PTT is used as a parameter for psycho-physiological stress monitoring in [13] and for arousal detection in sleep monitoring [24, 20].

A commonly used method for PTT calculation makes use of the *electrocardiogram* (ECG) and the *photoplethysmogram* (PPG), recorded simultaneously for one patient. The ECG sensor is mostly located on the patient's chest, while the PPG sensor is often placed near a finger. To connect both sensors, the majority of the available systems use cables. This approach is acceptable for stationary measurements but turns out to be impractical if patient mobility is given priority.

To overcome these limitations, we present a PTT monitoring system with dedicated ECG and PPG sensors, that communicate wirelessly. One of the main challenges is the exact time synchronization within the network. This is necessary to calculate precise PTT values.

Several groups work on implementing PTT or cuff-less BP measurements in wearable devices [26, 25, 21, 12]. As an example, Zhang et al. propose a health-shirt for long-term BP monitoring in [32]. Results are displayed on a wrist watch. [28] presents a hardware prototype for PTT based blood pressure measurements that uses Bluetooth to transmit the acquired data to a PDA-phone for calculation and visualization. [27] presents a wearable wrist device with manual PPG measurements and Espina et al. present a wireless PTT monitoring system that uses IEEE 802.15.4 [8, 9].

2. METHODS

2.1 Pulse Transit Time

As mentioned before, the PTT is the time, a BP wave needs to travel from the heart to a distant point of the body. Therefore, many PTT systems make use of an electrocardiograph and a photoplethysmograph to measure this time [6, 7, 13]. Another option is the utilization of bioimpedance sensors as done in [7]. We stick with the analysis of ECG and PPG signals for this work.

The typical curves of both examined signals are shown in Figure 1. The R-wave peak represents the electrical depolarization that results in the contraction of the heart, initiating a pressure wave that is released to the arteries. Therefore, the R-wave peak can be considered as the time of the starting pulse wave. The measurement of the arriving blood pressure wave at the distant point is done as follows: The generated PPG AC signal reflects the volume of blood located between the light emitter and the photo detector of the PPG sensor. The resulting curve, shown in the lower part of Figure 1, represents the passing by blood pressure wave.

Analyzing the existing literature, one can find several different points in the PPG signal used to calculate the PTT. Possible options are the minimum [7], the maximum, the point of maximum slope, a virtual base point [13] or 50% of the maximum [20]. We decided to use the point of maximum slope of the signal as it represents the maximum slope of the pressure signal as well and can be interpreted as the time of arrival of the pressure wave. Furthermore, this point is easy to detect.
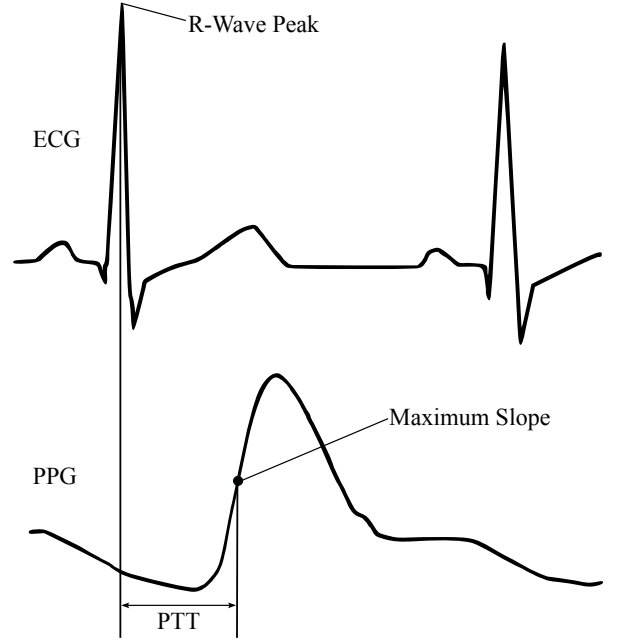

Figure 1: Calculation of the PTT defined as the time delay between the R-wave peak in the ECG and the characteristic point of maximum slope in the PPG.

To ensure minimal detection jitter even under harsh conditions like movement artifacts, weak signals or noise, we used a wavelet transform based fiducial point detection algorithm for ECG and PPG signals. These algorithms are described in section 2.5.1 in detail.

2.2 System Concept

The system was designed for a small group of people doing gymnastic exercises in a gymnasium. During their workout, several vital signs are recorded and analyzed. Figure 2 shows an overview of the projected system. It consists of two small devices per person and a central base station (coordinator). The first device is a two lead ECG monitor which is capable of sampling at 250 Hz. This ECG monitor is attached to a textile chest strap with integrated dry electrodes by several snap fasteners. The use of textile straps and dry electrodes turned out to be beneficial for several reasons. In contrast to the utilization of conventional adhesive electrodes, they can be easily applied by the patient without any help. Dry electrodes provide a sufficient signal quality for PTT analysis. Textile straps are convenient, even if used for several hours, and easy to clean.

The second device is a photoplethysmography sensor that utilizes a conventional finger probe. The red transmission signal is digitized at 250 Hz.

The desired system shall work for at least 16 hours without recharging the internal lithium polymer battery. The complete design cycle geared towards maximum energy conservation. This results in a hardware using ultra low power microcontrollers, an energy efficient wireless protocol and optimized sensor electronics.

Rather than transmitting the complete ECG and photoplethysmogram to the base station, the data is directly analyzed on the device using specialized algorithms which are
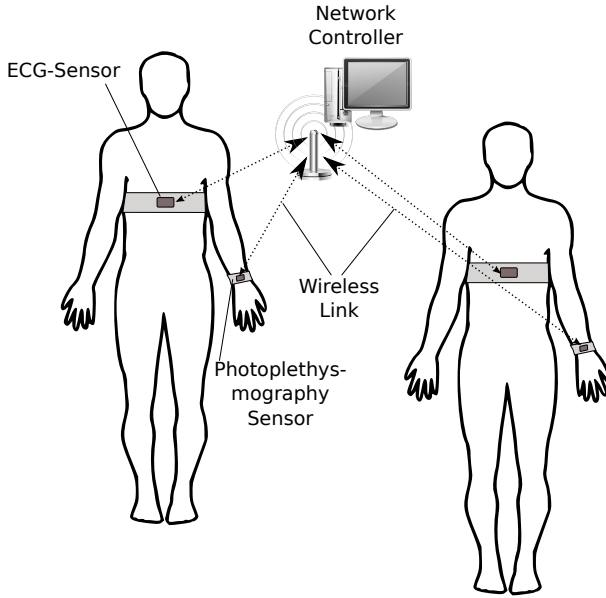
Figure 2: The concept of the wireless PTT monitoring system. ECG-sensors and PPG-sensors transmit time stamps of detected R-wave peaks and PPG peaks to the base station that calculates the PTT.
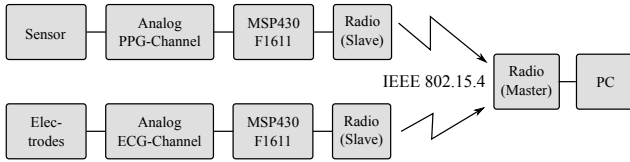

Figure 3: Building blocks of the wireless PTT-System.

executed on a microcontroller. To keep the network traffic low, only relevant results are periodically transmitted to the base station. This approach significantly reduces the energy consumption of the system since calculation costs are in general substantially smaller than transmission costs [16].

The final calculation of the PTT is carried out on the central base station, which might be a conventional personal computer. The results are displayed for each individual patient during the exercise in a "Live View" mode and are saved for further analysis. The resulting PTT graphs are enriched by additional data (acceleration, temperature, etc.) that is gathered by the two devices.

Figure 3 shows the hardware building blocks of the PTT system. The basic hardware layout of ECG and PPG devices is very similar. The sensor signals are amplified, filtered and conditioned in the analog front-end and finally digitized. The microcontroller runs the point detection algorithms and transmits the resulting time-stamps to the master.

2.3 Signal Acquisition

The acquisition of the plethysmography signal is presented schematically in the upper half of Figure 4. The electric current, generated by the photo diode of the sensor, is first transformed into a voltage and subsequently amplified and
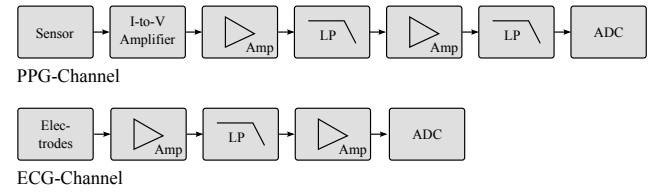

Figure 4: Schematic overview of the analog section of the sensor hardware.

low-pass filtered. Finally, the signal is sampled to be digitally processed.

Using standard sensors for pulse oximetry, the system is able to derive a plethysmography signal from the infrared or red channel. Depending on the type and placement of the sensor used, the quality of the signal generated by utilizing the different wavelengths varies. The current configuration of our prototypes makes use of the red channel. This is suitable for finger clip sensors.

The acquisition of the ECG signal is shown in the lower half of Figure 4. Two independent differential channels offer the possibility to switch channel in case of a noisy signal.

Both analog front-ends utilize software controlled dynamic offset correction and dynamic gain adaption to optimize signal quality. Our analog ECG channel supports a full dynamic range of up to $300\,\mu V$ at a 12 bit resolution ($73\,nV$ per digit). To our experiences, selecting a dynamic range of around $7\,mV$ ($1.7\,\mu V$ per digit) provides good results in most cases.

2.4 Radio Technology

The selection of an appropriate radio technology is one of the key aspects in the process of designing a mobile system with wireless connectivity. For a short range wireless body sensor network, the selection is limited to some standard candidates: WiFi, Bluetooth, IEEE 802.15.4 and Zig-Bee. Other proprietary radio technologies were not considered due to the lack of available hardware modules and high development and testing costs for a stack implementation.

Only recently, the small energy-per-bit values of modern WiFi solutions enables the usage of this technology in battery powered devices. Nevertheless WiFi is, from an energetic point of view, better suited for the transmission of large chunks of data than for the frequent transmission of very short messages as we intent to do. This is mainly due to the overhead for network management and the TCP/IP protocol.

While Bluetooth was used in several of our other body sensor network (BSN) projects (Inmusens [30], ECG-Vital [11], Well.com.e [3]), it can not be used here. The main reasons are the limitation to eight active devices per network and the comparatively high energy consumption for datagram transmission.

IEEE 802.15.4 [15] is a standard for low rate wireless personal area networks (LR-WPAN). The protocol was especially designed to provide small battery powered devices with a low energy consuming radio technology. IEEE 802.15.4 defines only the physical and MAC layer of the OSI reference model. The implementation of higher layers is in the responsibility of the user. For example ZigBee is based on the 802.15.4-PHY and -MAC and adds network, security and application layer functionality. These additional fea-
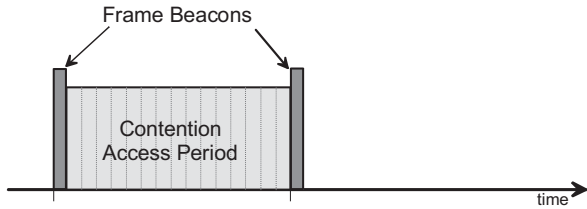
Figure 5: The superframe structure in a beacon enabled IEEE 802.15.4 network (from [15, p.18]).

tures are not needed for the projected network and would only introduce additional protocol overhead, resulting in a higher energy consumption. Finally, IEEE 802.15.4 ideally matched the requirements and was selected for this system.

The network operates at 2.4 GHz with a gross date rate of 250 kBit/s. All devices are organized in a star topology with the base station working as the 802.15.4 coordinator. The star topology is less complex than the peer-to-peer mode. All slave devices can only communicate with the PAN coordinator. The additional benefits of the optional peer-to-peer mode, like direct communication between devices or multi-hop communication are not necessary for the desired use case. Low energy consumption is the main design goal and the star network simplicity greatly contributes to its reduction.

The central base station is responsible for network management and especially maintains the central time base for the entire wireless network. None of the commercial available technologies provide time synchronization capabilities on the user level out of the box. To guarantee a reliable distributed PTT calculation, a maximum synchronization error of ± 1 ms is required. To archive this, a synchronization algorithm was implemented using the 802.15.4 beacon enabled mode.

Figure 5 shows the superframe structure of a beacon enabled 802.15.4 network. The superframe structure is bounded by beacon frames sent by the PAN coordinator and is divided into 16 equally sized slots [15]. Beacon frames are used to keep all connected network devices synchronized. The optional inactive period and guaranteed time slots (GTS) are not used in our configuration.

All slave devices can send data during the contention access period (CAP) using the slotted CSMA-CA mechanism. Devices that have nothing to send within the current superframe can enter the power down mode until the next beacon frame is expected. This further reduces their energy consumption.

To provide the user level time synchronization that is necessary for the generation of precise time stamps, the coordinator maintains a real time base with a 1 ms resolution. This real time value is transmitted in the payload field of every beacon. Before the transmission, the timer value is corrected using the internal 802.15.4 symbol counter with a $16\,\mu$s resolution to reduce the timing jitter introduced by the software stack. Beacons are sent every 983 ms (BeaconOrder = 6).

Whenever a slave device receives a beacon frame, it extracts the real time data and resets the its own time to the master time. Finally, a synchronization interrupt is triggered on the MCU using one of the external pins.

2.5 Algorithms

2.5.1 Fiducial Point Detection

The fiducial points from both, ECG and PPG, are extracted on the basis of the Wavelet Transform (WT).

WT basics: The WT breaks a time dependent signal $x(t)$ down into different scales a. The wavelet coefficients $X(a,t)$ are derived by comparing the signal to a scaled and translated wavelet ψ, i.e.

$$X(a,t) = \int_{-\infty}^{+\infty} x(\tau)\frac{1}{\sqrt{a}}\psi^*\left(\frac{\tau-t}{a}\right)d\tau. \quad a \in \mathbb{R}^*, \, t \in \mathbb{R}.$$

with $a \in \mathbb{R}^+$ and $t \in \mathbb{R}$. The different scales correspond to specific frequency ranges so that the WT acts as filter bank.

WT implementation: The numerical calculation of the WT bases upon a discretization of its parameters. The formulation

$$X(2^m, 2^m n) = \sum_{k=-\infty}^{+\infty} x(k)\frac{1}{\sqrt{2^m}}\psi\left(\frac{k}{2^m} - n\right) =: X(m,n)$$

with $m \in \mathbb{N}$ and $n \in \mathbb{Z}$ yields a dyadic, shift-invariant WT (D_yWT). In our implementation, the D_yWT is performed by applying the Algorithm à Trous [14]. Thereto, we apply the Quadratic Spline Wavelet [18]. This choice permits an implementation of the WT which exclusively relies on bit-shifts and summations. This renders our implementation useful for a real-time application under computational constraints. Details regarding the computational complexity can be found in [30].

Peak Detection: The peak detection follows the ideas of finding modulus maxima pairs in the wavelet coefficients across different scales which was, in the field of ECG processing, originally proposed by Li et al. [17]. Compared to Li et al. a simplified version was implemented which yields high accuracy while avoiding any back-searches [31]. In both, ECG and plethysmogram, the wavelet coefficients are compared to adaptive thresholds. The adaptation is based on previous detections and an actual noise estimate in the respective signal. The search for QRS complexes is carried out in scale $m = 2$ and $m = 3$, respectively. A removal of artifacts is done out by invoking the scale $m = 1$. Considering the plethysmogram, relevant peaks are detected in scale $m = 3$. The scale $m = 1$ is used to separate artifacts from physiological events.

As a result of processing, for both signals timestamps are generated which mark the occurrence time of QRS-complexes and plethysmography peaks, respectively. By that, the implemented processing steps guarantee for a high positive predictive value of found peaks in the ECG and PPG, respectively.

2.5.2 PTT Calculation

The base station receives data from many slave devices. As a first step, two corresponding devices must be paired using their ID and a known patient assignment.

For every device pair, the system keeps two queues of timestamps. One queue represents the detected ECG peaks and the other the detected PPG peaks.

Due to the block transfer of data packets, there is always a bulk of incoming peaks. In addition, peaks may be missing due to the impossibility of peak detection during heavy movement of the patient. This demonstrates, that not ev-
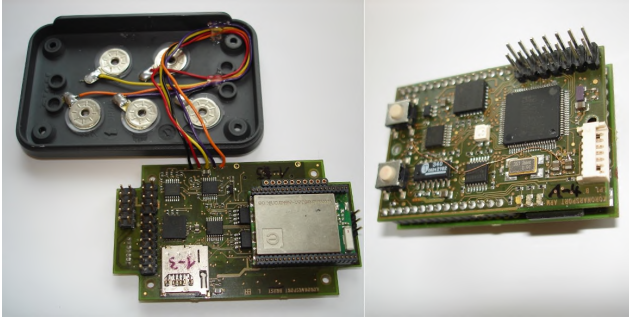
Figure 6: Printed circuit boards of the prototype hardware. The left side shows the ECG device and the case with snap fasteners, the right side shows the PPT sensor.

ery time stamp in one queue has necessarily a corresponding time stamp in the other queue.

PPG peaks are expected to succeed ECG peaks within an interval of 50 ms to 400 ms. The algorithm works as follows: Incoming data is a bulk of either PPG peaks or ECG peaks and is inserted into the corresponding queue. While both queues are not empty, the system continuously tries to match the two peaks at the head of the two queues.

If the time stamp of the current PPG peak lies before the time stamp of the current ECG peak, or their time difference is lower than 50 ms, no corresponding ECG peak could be found and the PPG peak is discarded. If the time difference of the ECG peak to the PPG peak passes a threshold (currently fixed to 400 ms) the system certainly missed a PPG peak and the ECG peak gets discarded. Whenever the time difference falls within the expected range, both peaks belong together and are removed from the queues. Their time difference is the wanted PTT.

3. RESULTS

3.1 Hardware Prototypes

The first prototypes of the ECG and PPG hardware can be seen in Figure 6. Both devices use the ultra low power microcontroller TI MSP430F1611 [29], running at 8 MHz.

The wireless connectivity is provided by an Atmel ATmega128RFA1 [2]. The ATmega128RFA1 is a 8-bit MCU with an integrated IEEE 802.15.4 transceiver for the 2.4 GHz band. The firmware of the transceiver module uses a customized version of the Atmel 802.15.4 MAC-Stack [1] and especially implements the time synchronization on user-level feature.

Each device is equipped with a micro SD card that is used to save firmware files and to buffer all data that could not be delivered to the base station in time due to interference, packet collision or while the sensor is out of range of the coordinator. Additionally, all recorded data can be saved to the card to keep raw data for potential analysis and algorithm optimization.

The modular firmware of the sensor nodes uses an embedded real time operating system. The code and the operational modes were optimized for low energy consumption. The sleep modes are used as often as possible to hit the operation time requirements. Additionally, the firmware of all

Figure 7: A pair of devices for the wireless PTT system in a typical configuration. The ECG recorder is worn around the chest using a textile strap, the PPG sensor around the arm.

processors can be updated over the air using the network management tool.

Figure 7 shows the final system as it will be used by the patient. The ECG sensor is attached to the textile strap containing dry electrodes. The PPG sensor is worn around the arm. Commercial finger probes can be used with our system.

Since the coordinator can not enter the sleep mode because the 802.15.4 inactive mode is not used, the base station is the device with the highest energy consumption. It has to receive and process the slave data and coordinate the time synchronization. Therefore, the base station is simply a small hardware module connected to the USB port of a conventional, wall-powered PC. This module consists only of the transceiver running a special base station firmware. Incoming data is simply forwarded to the network management tool, that has sufficient computational power to calculate and display the PTT.

The time synchronization was tested with the first ten prototype devices. An oscilloscope was connected to the synchronization pins of several spatially separated transceiver modules. The screen shot in Figure 8 shows the delay (synchronization error) between two devices. The histogram on the left side, calculated over 1000 beacon intervals, reveals synchronization error boundaries of around -600 μs and 400 μs. This is well within the desired range of ± 1 ms.

3.2 Measurement and Results

Figure 9 shows a short snippet of the signals generated by the two sensors. This record was taken using a special debug configuration of the sensor system. Using this operational mode, we were able to verify and optimize the signal acquisition of the sensors. When operating normally, nether the ECG nor the PPG curves are transmitted to maximize the energy conservation.

As the experimental setup, we used a subject, equipped with a set of prototype devices, on a bicycle ergometer.
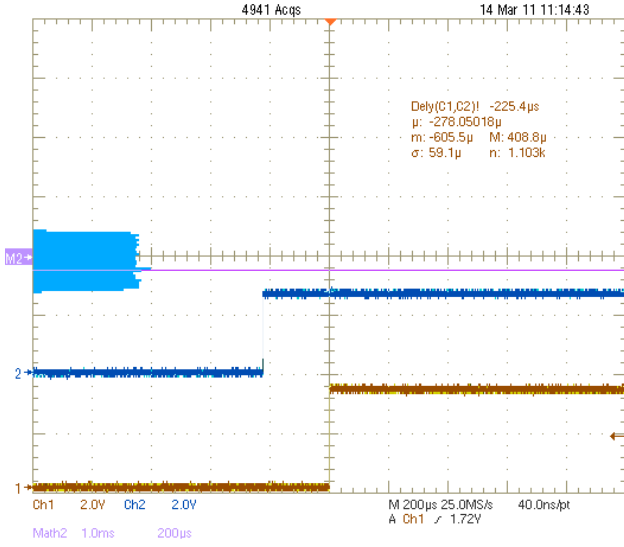
Figure 8: The oscilloscope screen shot shows the time difference measurement of two separate devices, synchronized by the network master. From the histogram on the left side we find the time delay uniformly distributed from -600 us to 400 us.

Table 1: Load levels on the ergomater during the different stages of the experiment.

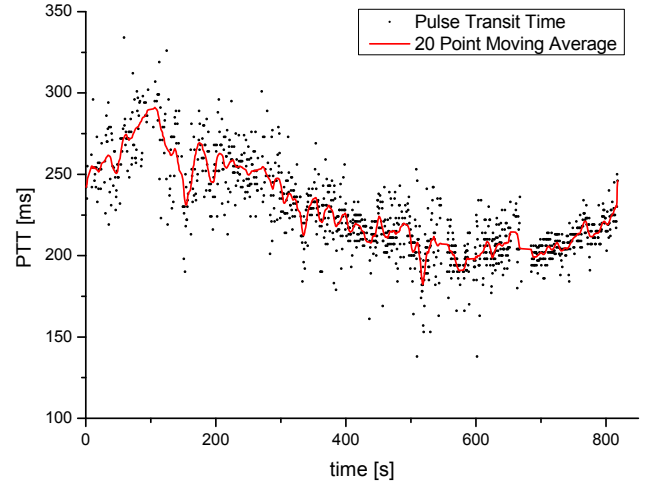| start time [s]	duration [s]	load level [W]
0	100	0
100	120	50
220	120	75
340	120	100
460	60	125
520	60	150
580	240	25

Figure 10: Results of the wireless PTT measurement experiment in that a subjects uses an ergometer with different load levels. Each point represents a valid PPT value.
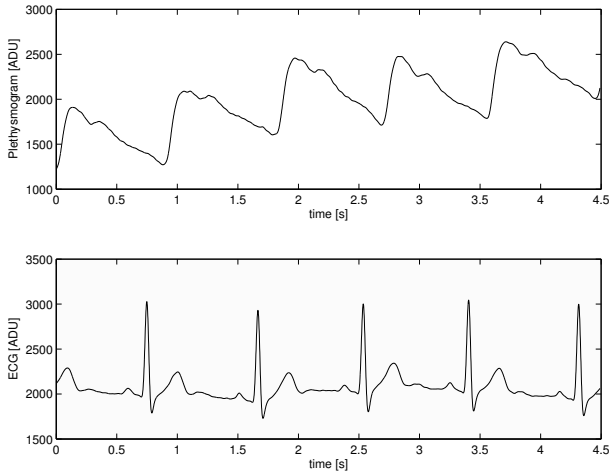

Figure 9: Extract of the PPG and ECG signals recorded with our hardware.

The coordinator was connected to a conventional PC that recorded and analyzed the received data.

The bicycle ergometer was programmed with rising load levels to increase the stress level of the subject, resulting in an increasing heart rate and blood pressure. We used load levels of up to 150 Watts. Table 1 documents the different phases of the experiment and the corresponding durations and load levels.

An advantage of a bicycle ergometer is the fixed relative elevation of the finger clip to the subject's heart. Additionally, the subject moves less than on a treadmill which would negatively affect the detection accuracy of the peaks.

Figure 10 shows the results of the experiment. Every measured PTT value is plotted over the time. One can notice a jitter in consecutive PTT values. Therefore, a 20 point moving average filter was applied to the data and the results were plotted as well.

The results show an increasing average PTT value for the first 100 s when the subject was, while sitting on the bicycle ergometer, regenerating from walking before. As the stress level of the subject is increasing, the average PTT is decreasing as expected. During the last four minutes of the experiment the subject regenerates and the average PTT value increases.

4. CONCLUSIONS AND FUTURE WORK

In this paper, we presented a wireless system for pulse transit time monitoring. This system is particularly suited for mobile applications since the hardware is not disturbing, easy to use and no cables are needed to connect the ECG sensor with the PPG sensor.

The presented system can be used to study PTT variations and might be helpful to further analyze the correlation function between blood pressure and PTT. The main benefits are precise and most notably continuous PTT values, that can be used to monitor direct responses to load level changes.

More complex and more robust methods for the determination of the time stamp of the arriving blood pressure wave from PPG signal are to be examined. This could result in less noise in the resulting PPT signal and so further improve the system.

One of the main directions of future work will be the reduction of hardware size to improve the usability. Furthermore, we want to carry out research regarding the detection of the most stable point within the PPG to improve the theoretical achievable accuracy. Another option is to change the sampling rate of the ECG and the PPG to 500 Hz or 1000 Hz to improve the accuracy of the calculated PTT signal. To do this, we need to switch to a more powerful MCU. Currently the used 250 Hz resolution is the upper limit for real time execution of the detection algorithms.

At the moment, we are designing a new PPG sensor that works without a finger probe but with a reflective sensor on the forehead. Our experiments showed, that the forehead is a good place for PPG measurements [22]. This position is less prone to movement artifacts than the extremities. While moving the arm up or down using a finger probe changes the PTT, the position (relative height) of the forehead sensor stays constant in relation to the heart.

The internal batteries of the next generation hardware will be charged wirelessly. By removing the charger plug opening, we are able to completely seal the hardware and make it splashproof. This greatly simplifies the process of cleaning and disinfecting the hardware what is an important feature for medical use.

Finally, we are testing systems that only consist of the ECG sensor and a PPG sensor. These systems are intended for personal use and work without a central base station. The ECG sensor will manage time synchronization, receive the PPG data and directly calculate the PTT. The results are written to the internal SD card and can be downloaded for later analysis.

5. REFERENCES

[1] Atmel. IEEE 802.15.4 MAC Stack Software, 08/10.

[2] Atmel. ATmega128RFA1: 8-bit AVR Microcontroller with Low Power 2.4GHz Transceiver for ZigBee and IEEE 802.15.4, 12/09.

[3] S. Beer and K.-L. Resch. Well.com.e: Entwicklung einer Gesundheitsplattform für proaktive, selbstbestimmte Menschen in der zweiten Lebenshälfte und ihre Dienstleister. In VDE Verlag, editor, *Ambient Assisted Living 2010*. VDE-Verl., Berlin, 2010.

[4] H. R. Black and W. J. Elliott. *Hypertension: A companion to Braunwald's heart disease*. Elsevier Saunders, Philadelphia, 2007.

[5] W. Chen, T. Kobayashi, S. Ichikawa, Y. Takeuchi, and T. Togawa. Continuous estimation of systolic blood pressure using the pulse arrival time and intermittent calibration. *Medical and Biological Engineering and Computing*, 38:569–574, 2000.

[6] C. Douniama and R. Couronne. Blood Pressure Estimation Based on Pulse Transit Time and Compensation of Vertical Position. In J. Hornegger, E. W. Mayr, S. Schookin, H. Feußner, N. Navab, Y. V. Gulyaev, K. Höller, and V. Ganzha, editors, *3rd Russian-Bavarian Conference on Biomedical Engineering*, volume 1, pages 38–41, Erlangen, 2007.

[7] C. Douniama, C. U. Sauter, and R. Couronne. Blood pressure tracking capabilities of pulse transit times in different arterial segments: A clinical evaluation. *2009 Computers in Cardiology*, pages 201–204, 2009.

[8] J. Espina, T. Falck, J. Muehlsteff, and X. Aubert. Wireless Body Sensor Network for Continuous Cuff-less Blood Pressure Monitoring. *2006. 3rd IEEE/EMBS International Summer School on Medical Devices and Biosensors*, pages 11–15, 2006.

[9] J. Espina, T. Falck, J. Muehlsteff, J. Yilin, M. A. Adan, and X. Aubert. Wearable body sensor network towards continuous cuff-less blood pressure monitoring. *2008. ISSS MDBS 2008. 5th International Summer School and Symposium on Medical Devices and Biosensors*, pages 28–32, 2008.

[10] J. E. Fischer and K. I. Bland. *Mastery of surgery*. Mastery of Surgery. Wolters Kluwer Health/Lippincott Williams & Wilkins, 2007.

[11] W. J. Fischer, H.-J. Holland, A. Heinig, and S. Zaunseder. 3-Kanal EKG-Gerät für die Langzeitüberwachung mit integrierter EKG-Vorauswertung und Bewegungsmustererkennung. In De Gruyter, editor, *Biomedizinische Technik*, volume Band 55 (Suppl. 1). 2010.

[12] W. B. Gu, C. C. Y. Poon, M. Y. Sy, H. K. Leung, Y. P. Liang, and Y. T. Zhang. A h-Shirt-Based Body Sensor Network for Cuffless Calibration and Estimation of Arterial Blood Pressure. *2009. BSN 2009. Sixth International Workshop on Wearable and Implantable Body Sensor Networks*, pages 151–155, 2009.

[13] S. Hey, A. Gharbi, B. von Haaren, K. Walter, N. Konig, and S. Loffler. Continuous Noninvasive Pulse Transit Time Measurement for Psycho-physiological Stress Monitoring. *Telemedicine eHealth*, pages 113–116, 2009.

[14] M. Holschneider, R. Kronland-Martinez, J. Morlet, and P. Tchamitchian. A Real-Time Algorithm for Signal Analysis with the Help of Wavelet Transform. In *Wavelets, Time-Frequncy Methods and Phase Space*. Springer Verlag, Berlin, 1989.

[15] IEEE. IEEE Standard for Information Technology-Telecommunications and Information Exchange Between Systems- Local and Metropolitan Area Networks- Specific Requirements Part 15.4: Wireless Medium Access Control (MAC) and Physical Layer (PHY) Specifications for Low-Rate Wireless Personal Area Networks (WPANs). *IEEE Std 802.15.4-2006*

(*Revision of IEEE Std 802.15.4-2003*), pages 1–305, 2006.

[16] H. Karl and A. Willig. *Protocols and architectures for wireless sensor networks*. Wiley, Chichester, reprinted with corr. edition, 2007.

[17] C. Li, C. Zheng, and C. Tai. Detection of ECG characteristic points using wavelet transforms. *IEEE Transactions on Biomedical Engineering*, 42(1):21–28, 1995.

[18] S. Mallat and S. Zhong. Characterization of signals from multiscale edges. *Pattern Analysis and Machine Intelligence, IEEE Transactions on*, 14(7):710–732, 1992.

[19] D. B. McCombie, A. T. Reisner, and H. H. Asada. Motion based adaptive calibration of pulse transit time measurements to arterial blood pressure for an autonomous, wearable blood pressure monitor. *2008. EMBS 2008. 30th Annual International Conference of the IEEE Engineering in Medicine and Biology Society*, pages 989–992, 2008.

[20] R. P. P Smith, J. Argod, J.-L. Pepin, and P. A. Levy. Pulse transit time: an appraisal of potential clinical applications. *Thorax*, 54(5):452–457, 1999.

[21] P. Pandian, K. Mohanavelu, K. Safeer, T. Kotresh, D. Shakunthala, P. Gopal, and V. Padaki. Smart Vest: Wearable multi-parameter remote physiological monitoring system. *Medical Engineering & Physics*, 30(4):466–477, 2008.

[22] S. Päßler and M. Pietzsch. Entwicklung, Aufbau und Erprobung eines mobilen Pulsoximeters für reflexive und transmissive Sensoren mit aktiver Unterdrückung von Bewegungsartefakten, *Diploma Thesis*, 2009, Fraunhofer IPMS.

[23] R. A. Payne, C. N. Symeonides, D. J. Webb, and S. R. J. Maxwell. Pulse transit time measured from the ECG: an unreliable marker of beat-to-beat blood pressure. *J Appl Physiol*, 100(1):136–141, 2006.

[24] D. Pitson, N. Chhina, S. Knijn, M. van Herwaaden, and J. Stradling. Changes in pulse transit time and pulse rate as markers of arousal from sleep in normal subjects. *Clinical science (London, England : 1979)*, 87(2):269–273, 1994.

[25] C. C. Y. Poon, Y. M. Wong, and Y.-T. Zhang. M-Health: The Development of Cuff-less and Wearable Blood Pressure Meters for Use in Body Sensor Networks. *2006. IEEE/NLM Life Science Systems and Applications Workshop*, pages 1–2, 2006.

[26] C. C. Y. Poon and Y. T. Zhang. Cuff-less and Noninvasive Measurements of Arterial Blood Pressure by Pulse Transit Time. *2005. IEEE EMBS 2005. 27th Annual International Conference of the Engineering in Medicine and Biology Society*, pages 5877–5880, 2005.

[27] D.-W. Ryoo, C.-S. Bae, and J.-W. Lee. The Wearable Wrist-Type Gadget for HealthCare based on Physiological Signals. *2008. ICCE 2008. Digest of Technical Papers. International Conference on Consumer Electronics*, pages 1–2, 2008.

[28] F. E. Tay, D. Guo, L. Xu, M. Nyan, and K. Yap. MEMSWear-biomonitoring system for remote vital signs monitoring. *Journal of the Franklin Institute*, 346(6):531–542, 2009.

[29] Texas Instruments. MSP430F1611 - 16-bit Ultra-Low-Power MCU.

[30] S. Zaunseder, W. J. Fischer, S. Netz, R. Poll, and M. Rabenau. Prolonged Wearable ECG Monitoring - a Wavelet Based Approach. *2007 IEEE Sensors*, pages 1197–1200, 2007.

[31] S. Zaunseder, F. W.-J., P. Rüdiger, and M. Rabenau. Wavelet-Based Real-Time ECG Processing for a Wearable Monitoring System. In P. Encarnação and A. Veloso, editors, *Proceedings of the First International Conference on Biomedical Electronics and Devices, BIOSIGNALS 2008, Funchal, Madeira, Portugal, January 28-31, 2008, Volume 2*, pages 255–260. INSTICC - Institute for Systems and Technologies of Information, Control and Communication, 2008.

[32] Y.-T. Zhang, C. C. Y. Poon, C.-h. Chan, M. W. W. Tsang, and K.-f. Wu. A Health-Shirt using e-Textile Materials for the Continuous and Cuffless Monitoring of Arterial Blood Pressure. *2006. 3rd IEEE/EMBS International Summer School on Medical Devices and Biosensors*, pages 86–89, 2006.